

A New Approach for Face Detection based on Photoplethysmographic Imaging

He Liu^{1, 2}, Tao Chen¹, Qingna Zhang¹, and Lei Wang^{1*}

¹Shenzhen Institutes of Advanced Technology, Chinese Academy of Sciences, China

²Haerbin Institute of Technology, China

Email: he.liu@siat.ac.cn; wanglei@siat.ac.cn

Abstract. Face detection as a necessary first-step has been widely used in face recognition systems and many other applications. However, many effective face detection methods still stay in grayscale images. Nowadays, photoplethysmographic imaging (PPGi) for cardiovascular and hemodynamic analysis has become an attractive research area and pulsatile signal extracted from skin surface can be obtained using a digital camera under the condition of the ambient light. In this paper, we introduce a new approach of face detection based on the PPGi technology. First, a reference signal is required to calculate the standard value of the subject's heart rate. The frame images are sliced into many small regions and the frequency of every region is estimated, respectively. According to the predetermined threshold between the standard value and the calculated value, an index of the existence of the face region can be created. And then the binary image of the face region can be formed. Finally, an elliptical template can be formed using the edge information of the binary image. In the condition of different heart rate, we can obtain effective results.

Keywords: face detection; grayscale images; photoplethysmographic imaging; heart rate

1 Introduction

In the last decades, face detection is a rapidly growing research area. With the purpose of locating and extracting the face region from the backgrounds, many efficient face detection methods based on skin color characteristics have been proposed [1-4]. Face detection also has several applications in many areas such as video coding, video conferencing, content-based image retrieval, crowd surveillance and intelligent human-computer interfaces. The human face is a dynamic object and has a great variability in its appearance, which makes face detection become a difficult problem in computer vision and many other applications. In order to improve the accuracy of face detection, some efficient methods have been developed. Traditionally, methods that focus on facial landmarks (such as eyes, nose etc), that detect face-like colors in circular regions, or that use standard feature templates, were used to detect faces. However, these attempts don't improve the accuracy of face detection fundamentally. Face detection is still a challenge because of several difficulties, such

as variable face orientations, different face sizes, partial occlusions of faces in an image, and changeable lighting conditions.

Photoplethysmography imaging (PPGi) as a new research field is used to extract physiological information in recent years. As a fact that volume of the blood in the blood vessels is constantly changing during the cardiac circulation system and human face is a part of a living body, we can learn that there is a constant blood flow in the subject's face region. Photoplethysmography (PPG) corresponds to the variations in reflected light due to cardiovascular blood volume pulse [5]. Nowadays, it has been shown that heart rate (HR) could be measured from human face with a simple consumer level digital camera under ambient light [6]. The noncontact methods to estimate HR can obtain very high accuracy.

In this paper, we propose a new methodology of face detection based on PPGi technology. The pulsatile signal extracted from face as a unique feature may be used to improve the robustness of noncontact face detection. The frame images obtained from the recorded video stream are sliced equally into many small regions. Then the frequency of every region is estimated, respectively. According to the predetermined threshold between the standard value and the calculated value, an index of the existence of the face region can be created. Because the human face can be approximate to an elliptical area, we use the edge information of the binary image of the subject's face region to fit out an accurate face region.

2 Method

2.1 Experimental Setup

We use a digital camera to record the videos of the subjects of our research team for analysis the information of the physiological signals. All videos were recorded in color (24-bit RGB with 3 channels \times 8 bit/channel) at 30 frames per second (fps) with pixel resolution of 640×480 and saved in AVI format on the laptop. A total of ten healthy volunteers (eight males, aged from 24 to 35 with a mean age of 28.6 years; two females, both aged 25 years old), recruited from the Shenzhen Institutes of Advanced Technology, Chinese Academy of Sciences, were enrolled in this study.

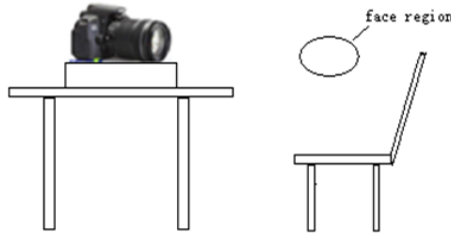


Fig. 1. shows the specific experimental environment when recording the subject's videos

Fig. 1 shows the experimental setup. Our experiments were conducted indoors and with the ambient light as the only source of illumination. The subjects were asked to seat at a desk in front of a digital camera at a distance of approximately 0.4 m from the

camera lens and to keep normal breathing. The experiment procedure has three sessions for all subjects. In session 1, the subject is the state of rest. In session 2, the subject is the state after gentle exercise. In session 3, the third one is the state after intense exercise.

2.2 Frame Image Acquisition and Processing

In order to detect the subject's face region in our experiments, we use the technology of division the video streaming to obtain the single frame image sequence at 30 Hz. And then each image was equally divided into many small regions. The size of these small regions is 40×30 pixels. Image processing was performed with custom software written in Matlab, Mathworks. The result of the divided small region can be seen in Fig. 2. According to established theoretical model [7], physiological processes of heart pulsation lead to modulation in time of fractional blood volume at the heart-beat rate. Modulation of the blood volume results in the absorption modulation of the light penetrated in the skin, which leads to the intensity modulation of light reflected in vivo from the subject's skin. Therefore, the value of pixels with the same spatial coordinates (x, y) in series of recorded frames is also modulated in time with the heart-beat rate. This fact was confirmed in numerous experiments including those carried out recently with digital cameras in the reflection mode [8].

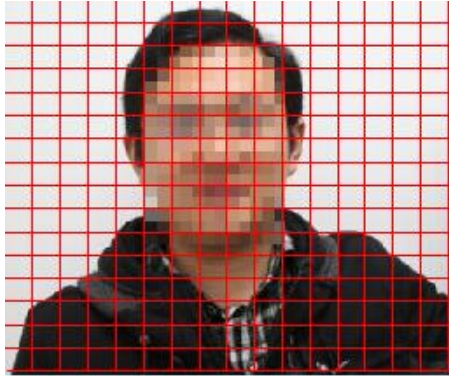


Fig. 2. The result of the divided small region.

By recording a video of the facial region with a digital camera, the RGB channels pick up a mixture of the reflected pulsatile signal along with other sources of fluctuations in light due to motion artifacts. So each color sensor records a mixture of the original source signals with slightly different weight. For each frame image, the total number of the small regions is 16×16 . Then the R, G, B channel of each small region of the images will be extracted. After these processing steps, all pixel values within each small region were spatially averaged to form a red, green and blue measurement point. After the spatial averaging operation, we can obtain the raw signal $x(t)$ of the G channel within the duration of the recorded video. In the previous literatures [6, 9], it is demonstrated that the result of G channel is better than the result of R channel and B channel when calculating the subject's HR. For the sake of simplicity, we always selected the G channel as the desired signal for further analysis.

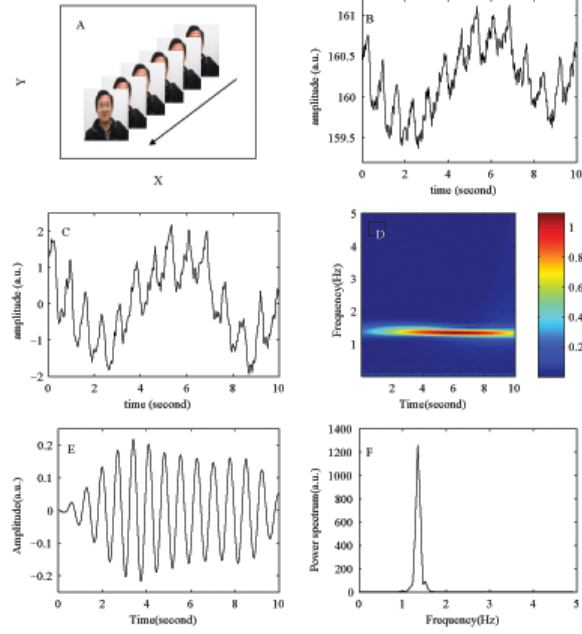


Fig. 3. The result of the reference signal. (a) The result of the frame images. (b) The result of the raw trace of the G channel of the RGB image. (c) The result of the processed signal. (d) The result of the Wavelet Transform. (e) The result of the reconstructed signal. (f) The result of the power spectrum of the reconstructed signal.

2.3 Reference Signal Formation

In order to analysis the characteristic of the pulsatile signal of the subjects, we firstly process the recorded video frames to generate a reference signal. We select the forehead area of the subjects as the region of interest (ROI) in our research to generate a reference signal. And then, the bounding box containing the forehead regions of the subjects were selected at the first frame of the recorded video. Coordinates of the selected forehead region remained the same for the whole sequence of the frame images in Fig. 3a. All pixel values within the selected ROI were spatially averaged resulting in a single mean value of each recorded frame. Time-trace of this mean value during the whole recorded video is shown in Fig. 3b. In Fig. 3b, we can see that the signal is a kind of time-varying signal. We want to obtain the frequency spectral characteristic of the time-varying signal, so we should transform the time-varying signal from time domain to frequency domain. As we can see from Fig. 3d, it was obtained by applying wavelet transform to the signal shown in Fig. 3c. Fig. 3e shows the reconstructed signal using the coefficients of the wave transform. Typical power spectrum curve of wavelet transform coefficients of the mean-pixel value of the located ROI is shown in Fig. 3f.

2.4 Signal Processing

In this study, interest of the underlying signal is the pulse wave of the cardiovascular. Signal processing is a key step for extracting the human body's physiological parameters. In our research, we use continuous wavelet transform (CWT) to filter the pulse signal. The CWT constructs a time-frequency representation of a signal and has been used to denoise or refine peaks [10] and significant points [11] in PPG signals. Inner product was used in continuous wavelet transform to measure the similarity between an analyzing function and a signal. Due to the width of the window is constantly changing when calculating the wavelet transform coefficients, so the continuous wavelet transform can detect the rapid changes in both time domain and frequency domain. This is the most significant advantage of wavelet transform when comparing to the Fourier transform and the short time Fourier transform. Many advantages have resulted in CWT being increasingly used for biological signals analysis [12, 13]. The non-stationary PPG signal is convolved with a child wavelet $\psi_{\tau,s}$, representing a scaled and shifted version of a mother wavelet ψ :

$$CWT_x^\psi(\tau, s) = \int_{-\infty}^{\infty} x(t) \psi_{\tau,s}(t) dt \quad (1)$$

$$\psi_{\tau,s}(t) = \frac{1}{\sqrt{|s|}} \psi\left(\frac{t-\tau}{s}\right) \quad (2)$$

where $\psi_{\tau,s}$ is the child wavelet, scaled by s and dilated by τ . ψ is the alleged mother wavelet. There is a relationship between analyzed frequencies and the scale parameter when we use wavelet transform to process signal problem. Decreasing s and shrinking the wavelet size results to cover a smaller signal in the time domain, leading to analyze higher frequencies and vice versa. According to the input signal properties and different application scope, we can choose different wavelet functions from a large set of standard mother wavelets for further analysis. The cmor3-3 wavelet has already been used to analyze PPG signals [14] and was employed in this study. The original signal can be reconstructed from the wavelet transform via the following inverse equation:

$$x(t) = \frac{1}{C_\psi} \int_0^\infty \int_{-\infty}^\infty \frac{1}{s^2} CWT_x^\psi(\tau, s) \frac{1}{\sqrt{|s|}} \psi\left(\frac{t-\tau}{s}\right) d\tau ds \quad (3)$$

$$C_\psi = \int_0^\infty \frac{|\psi'(\xi)|}{|\xi|} d\xi < \infty \quad (4)$$

where C_ψ is the admissibility condition and ψ' is the Fourier transform of ψ . The DC component is removed to reveal detailed information [15] on lower scales prior to performing the CWT. The equation as follows:

$$X_{AC}(t) = \frac{x(t) - \mu}{\sigma} \quad (5)$$

where μ and σ represent the mean value and standard deviation of the raw PPG signal $x(t)$. The waveform of the reference signal $X_{AC}(t)$ is shown in Fig. 3c. The CWT is then computed within an operational frequency band, set to [0.8, 2.0] Hz corresponding to 48-120 beat per minute.

The wavelet energy curve can be used to filter the wavelet transform coefficients, its maximum value in the frequency axis corresponding to the averaged HR. The pulse wave presents stronger amplitudes than those generated by noise and trends. A weighted product is applied between the energy curve and the CWT coefficients. And then, we use the inverse wavelet transform represented as Eq. 4 to reconstruct a de-noised version of the raw signal. The cascade of these two operations-weighting the CWT and reconstructing the signal by inverse CWT - is employed to filter the PPG signal in the operational band [0.8, 2.0] Hz [16].

2.5 Define a 4-neighbourhood of the Divided Image Pixel Block

In image processing, 4-neighbourhood of the pixel as a basic concept has become one of the most common principles to determine whether the pixels are connected or not. In our research, we want to detect the appropriate regions to form a map of the subjects' HR. According to the concept of the 4-neighbourhood of the single pixel, we define a concept of the 4-neighbourhood of the divided small image pixel block. Accordingly, the custom 4-neighbourhood of the divided small image pixel block can be seen in Fig. 4.

	B1	
B2	B0	B4
	B3	

Fig. 4. The schematic plot of 4-neighbourhood. The function of the 4-neighbourhood is to detect the connectivity of the pixel block.

2.6 The method of obtaining the proper boundary of the face image

In order to obtain the useful information of each small image in our study, we applied fast Fourier transform to the reconstructed reference signal and the processed signal of each small region to obtain the frequency information. For the reference signal and the processed signal, the maximum value around 1.0 Hz can be read from the frequency-amplitude curve. After this step, a mathematical expression can be represented as Eq. 6 to calculate the result of the heart beats per minute. The specific mathematic expression as follows:

$$Value = f \times 60 \quad (6)$$

In Eq.6, the parameter *Value* represents the result of the heart beats per minute, and the parameter *f* represents the frequency of the reference signal and the processed signal.

Next, we calculate the result of each small image pixel block to preliminary locating the rough ROI. In this step, we define a threshold ξ ($\xi = 3$) to determine whether

the detected area is appropriate or not. The specific mathematic expression as follows:

$$V_i = \begin{cases} f_i, \|f_i - std\| \leq \xi \\ 0, \|f_i - std\| \geq \xi \end{cases} \quad i = 1, 2, 3, \dots, N \quad (7)$$

for each i , we get a value of the subject's HR. The symbol f_i represents the value of the HR of each detected small region, parameter std represents the result of the subject's HR calculated by the reference signal and N represents the total number of the small image block. If the result of the heart-beat per minute of the subject meets the upper criteria of the Eq. 7, we will use the value as the effective heart-beat value of the subject. If not so, we will set the value to zero. This step can help us obtain the rough scope of the effective face region.

In order to further locating the ROI accurately, we use the function of the custom 4-neighbourhood to decide whether take the small region as an effective area or not. For each small image pixel block, the traversal algorithm of the 4-neighbourhood is used to obtain the most suitable regions of the frame image. And then, the values returned from the algorithm to form a map of detected regions of interest. After these processing steps, the results of the candidate region have been calculated.

Now, we introduce the judgment criterion of the connectivity of the divided small pixel block. As can be seen in Fig. 4, if the value of the image pixel block B0 meets the upper criteria of the mathematic Eq. 7, and there are at least two values of the image pixel block B1、B2、B3、B4 meet the upper criteria of the mathematic Eq. 7, too. We will mark the area B0 as the regions of interest in our research. The rest results can be processed using the same method. If not so, we will delete the area and set the value to 0. Accordingly, the located rough scope of the subject's face region with different states can be seen in Fig. 5.

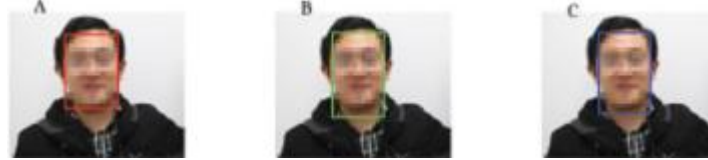


Fig. 5. The rough scope of the face region.

2.7 The Method of Obtaining the Binary Image

After determining the value of the HR of each small area, the rough boundary of the face region can be obtained. In order to reach the goal that locating an elliptical face region, we should obtain the binary image. Next, we introduce the method to obtain the binary image. For each detected small area, we will set all pixels value to 1 if the value of the HR greater than zero. Accordingly, we will set all pixels value to 0 if the value of the HR equals to zero. The expression can be written as Eq. 8.

$$P_i = \begin{cases} 1, V_i > 0 \\ 0, V_i = 0 \end{cases} \quad i = 1, 2, 3, \dots, N; j = 1, 2, 3, \dots, M. \quad (8)$$

For each i , the pixels value of the small region can be computed. The symbol V_i

represents the value of each small detected area. The symbol P_i represents the pixel value of each small detected area. N and M represents the total number of the small image block and the total number of the pixels of each small image block respectively.

2.8 The method of ellipse fitting

Robert operator is one of the most commonly used algorithms of the image edge detection. In this research, we use Robert operator to obtain the edge information of the binary image. After this step, the values of the edge of the binary image are equal to 1. According to the position of x-coordinate and y-coordinate of all the value 1, an optimal ellipse fitting function named fitellipse is used to calculate the parameters of the ellipse. These parameters can be marked as $A = (C_x, C_y, R_x, R_y, \theta)$. The parameters (C_x, C_y) , (R_x, R_y) , and θ represent the center coordinates, the length of the semi-major axis and short half shaft, and the rotation angle of the ellipse respectively. The input variables of the optimal ellipse fitting function are vector \mathbf{x} and vector \mathbf{y} . Vector \mathbf{x} and vector \mathbf{y} can be calculated by Eq. 9. The output results of the optimal ellipse fitting function are the parameters which meet the coordinate distribution of the vector \mathbf{x} and vector \mathbf{y} . The relationship between the coordinate position (x, y) and each parameter of A can be expressed as Eq. 9.

$$\begin{cases} x = R_x \times \cos \alpha \times \cos \theta - R_y \times \sin \alpha \times \sin \theta + C_x \\ y = R_y \times \cos \alpha \times \sin \theta - R_x \times \sin \alpha \times \cos \theta + C_y \end{cases}, 0 \leq \alpha \leq 2\pi \quad (9)$$

According to the results returned from the function of fitellipse, an ellipse which is very similar to the shape of the face region can be drawn using a function written in ellipse.

2.9 Statistics

Box plot can be used to detect the outlier of the experimental results. In the process of slicing the video frame image into small regions, we are not able to determine the position of the eyebrows, beard and eyes precisely. So the map of detected face region could contain false values when comparing to the standard result of the subject's HR. In order to judge whether the detected face region is reasonable or not, we drawing the box plots to show the outlier of the proposed methodology which used to locate the rough scope of the face region.

3 Results

The key point of this paper is how to locate an accurate face region based on the result of the subject's HR. So calculating the HR of the subject is the most crucial step. In order to validate the correctness of the calculated result, a reference signal formed from the same frame images. Table 1 shows the calculated result of each small area. As can be seen from Table 1, the result contained two abnormal values

(the number 0 lies in the row 5, column 7 and column 9 represent the abnormal result). But these error values are acceptable. The results of the subjects' HR of different state can be seen in Table 2.

Table 1 The map of the detected area. The light blue numbers represent the clustering characteristics of the face region, the numbers 0 lie in the row 5, column 7 and column 9 represent the abnormal result, the numbers 78 and 81 lie in the row 7, column 11 and row 13, column 9 respectively do not meet the definition of the 4-neighbourhood of the divided image pixel block.

0	0	0	0	0	0	0	0	0	0	0	0	0	0	0	0
0	0	0	0	0	0	0	0	0	0	0	0	0	0	0	0
0	0	0	0	0	0	78	81	81	78	0	0	0	0	0	0
0	0	0	0	0	78	81	81	81	81	0	0	0	0	0	0
0	0	0	0	0	78	0	81	0	84	0	0	0	0	0	0
0	0	0	0	0	78	84	84	81	78	0	0	0	0	0	0
0	0	0	0	0	81	81	81	84	84	78	0	0	0	0	0
0	0	0	0	0	81	84	81	81	84	0	0	0	0	0	0
0	0	0	0	0	0	84	81	81	81	0	0	0	0	0	0
0	0	0	0	0	0	81	81	78	84	0	0	0	0	0	0
0	0	0	0	0	0	78	81	84	78	0	0	0	0	0	0
0	0	0	0	0	0	0	81	84	0	0	0	0	0	0	0
0	0	0	0	0	0	0	0	81	0	0	0	0	0	0	0
0	0	0	0	0	0	0	0	0	0	0	0	0	0	0	0
0	0	0	0	0	0	0	0	0	0	0	0	0	0	0	0
0	0	0	0	0	0	0	0	0	0	0	0	0	0	0	0
0	0	0	0	0	0	0	0	0	0	0	0	0	0	0	0

Table 2 The results of the subjects' heart-beats with different states. State 1 represents the state of rest, state 2 represents the state after gentle exercise, and state 3 represents the state after intense exercise.

Subject number	State 1(bpm)	State 2(bpm)	State 3(bpm)
Subject 1	81±3	89±3	96±3
Subject 2	75±3	81±3	90±3
Subject 3	89±3	96±3	105±3
Subject 4	65±3	70±3	81±3
Subject 5	73±3	79±3	92±3
Subject 6	69±3	76±3	85±3
Subject 7	93±3	101±3	112±3
Subject 8	78±3	85±3	95±3
Subject 9	71±3	80±3	93±3
Subject 10	85±3	93±3	104±3

In order to obtain the binary image of the face region, the method described in the previous section (The method of obtaining the proper boundary of the face image) was used to calculate the position of up, down, left and right boundary scope of the face region. The result of the rough scope of the detected face region with different states can be seen in Fig. 5. In Fig. 6, we use the box plot to detect the outlier of the subject's HR. Fig. 6a represents the box plot of the HR with the state of rest. Fig. 6b

represents the box plot of the HR with the state after gentle exercise. And Fig. 6c represents the box plot of the HR with the state after intense exercise. After this step, the outliers of the subject's HR can be detected. If the outliers are reasonable, the binary image of the face region with different state can be obtained. And then, the ellipse fitting function was applied on the edge image processed by the Robert operator to return the optimal elliptic parameters. Using these parameters returned from the ellipse fitting function, the result of the detected face region with different state can be seen in Fig. 7.

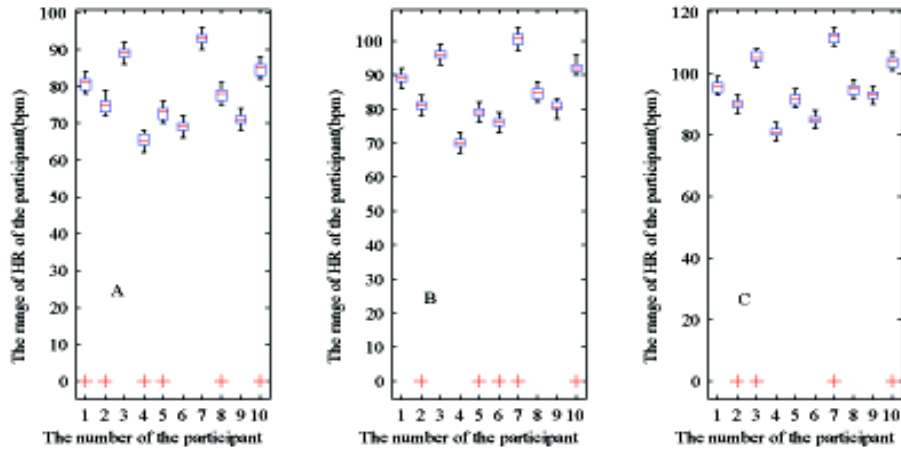


Fig. 6. The box plot of the heart rate with different states. (a) The box plot of the heart rate with the state of rest. (b) The box plot of the heart rate with the state after gentle exercise. (c) The box plot of the heart rate with the state after intense exercise.

4 Discussion

In this study, we detect the face region based on PPGi. Before recording the video, the subject was asked to find a comfortable position, and to breathe normally. In recent years, many scholars have proposed many efficient and robust face detection algorithm. However, these algorithms are based on color information. PPG is a non-invasive optical method to detect a cardiovascular pulse wave travelling through the human body. The basic form of PPG technology requires only two optoelectronic components: a light source to illuminate a part of the human body and a photo-detector to measure small variations in light intensity after light interaction with the illuminated part. The core of our method is based on the blood flow characteristic in a living body. As proposed in this research, in order to obtain an accurate signal to calculate the result of the subject's HR, we use the wavelet transform to remove noise from the raw photoplethysmographic signal of the G channel of the RGB image. This step is quite critical for subsequent processing. The result of the reference signal obtained from the same frame image can help us getting the correct calculated result for further analysis.

In Fig. 5, we can clearly see that the neck is also included in the detected face re-

gion. In our research, we found that we can detect the subject's HR in a small region. The size of the small region is $\text{width} \times \text{height} = 30 \times 40$ pixels. However, the size of the subject's neck is larger than the small region. So the detected region would contain the subject's neck. And the detected face with the ratio range between 0.7 and 2.1 is reasonable.

According to Eq. 6 and Eq. 7, a map of the detected area can be formed. Because of the influence of the eyes, beard and eyebrows, we can see a little abnormal result in Fig. 6 (the red + represents the abnormal number 0). In order to locate the face region accurately, we use the 4-neighbourhood of the divided small image pixel block to make a best decision. So the abnormal result would be contained in the map of the detected area. In order to obtain an accurate binary image, the morphological operation method and the hole filling method were adopted to process the area of the abnormal result. The method of obtaining the binary image proposed in this paper is different from the method of converting color space using the gray threshold. If the result of the subject's HR meets the upper criteria of the Eq. 7 and the connectivity of the 4-neighbourhood of the pixel block respectively, we will set all the pixel values of each small area to 1. So the result of our method would not contain many small holes phenomenon cause by the inconsistent color information.

After obtaining the edge information of the binary image, the coordinate position of the value 1 can be calculated in the rough scope of the image. Then we use the coordinate position as the input variable of the fitellipse function to calculate the parameters of the ellipse template. The result of the detected face region is effective with different states. After this research, we have found that the information of the subject's HR may be suit for emotion recognition and mental stress evaluation. For further study, we should research the potential value of the information of the HR in many other application fields.

5 Conclusions

In this paper, we have described and evaluated a novel methodology for face detection from video recordings of the human face and demonstrated an implementation using a digital camera with ambient daylight providing illumination. Wavelet transform plays an important role in removing noise and signal reconstruction. In order to locate the rough scope of the subject's face region, the custom 4-neighbourhood of the divided small image pixel block can help us to make a best decision. According to Eq. 8, we can obtain an accurate binary image. Obtaining the accurate binary image is a critical step for detecting the precise face region. We can draw a conclusion that our method based on the information of the HR has a very high precision.

Acknowledgment

This work was financed partially by the National 863 Program of China (Grant No. 2012AA02A604), the Next generation communication technology Major project of

National S&T (Grant No. 2013ZX03005013), the Key Research Program of the Chinese Academy of Sciences.

References

1. O. Jesorsky, K. J. Kirchberg, and R. W. Frischholz, "Robust face detection using the hausdorff distance," The third International Conference on Audio-and video-based biometric person authentication, Springer, Lecture Notes in Computer Science 2011, 2001, pp. 90-95.
2. P. Viola, and M. J. Jones, "Robust real-time face detection," Computer vision 2004, 57(Suppl 2), pp. 137-154.
3. W. C. Hu, C. Y. Yang, D. Y. Huang, and C. H. Huang, "Feature-based face detection against skin-color like backgrounds with varying illumination," Information Hiding and Multimedia Signal Processing 2011, 2(Suppl 2), pp. 123-132.
4. A. P. Chen, L. Pan, Y. B. Tong, and N. Ning, "Face detection technology based on skin color segmentation and template matching," Education Technology and Computer Science (ETCS). Second International Workshop on IEEE 2010, 2: pp. 708-711.
5. J. Allen, "Photoplethysmography and its application in clinical physiological measurement," Physiological Measurement 2007, vol. 28, pp. R1-39.
6. W. Verkrusse, L. O. Svaasand, and J. S. Nelson, "Remote plethysmographic imaging using ambient light," Opt. Express 16 (26), 21434-21445 (2008).
7. W. J. Cui, L. E. Ostrander, and B. Y. Lee, "In vivo reflectance of blood and tissue as a function of light wavelength," IEEE Trans Biomed Eng 1990, 37 (Suppl 6), pp. 632-639.
8. M. Z. Poh, D. J. McDuff, and R. W. Picard, "Non-contact, automated cardiac pulse measurements using video imaging and blind source separation," Opt. Express, vol. 18, No.10, 10 May 2010.
9. H. Liu, Y. Wang, and L. Wang, "The Effect of Light Conditions on Photoplethysmographic Image Acquisition Using a Commercial Camera", vol. 2, 2014.
10. Soni S, and Namjoshi Y, "Delineation of Raw Plethysmograph using Wavelets for Mobile based Pulse Oximeters," Proceedings of 5th Innovative Conference on Embedded Systems, Mobile Communication and Computing 2010, pp. 74-84.
11. T. Peterek, M. Prauzek, and M. Penhaker, "A new method for identification of the significant point in the plethysmographical record," Proc. 2nd International Conference on Signal Processing Systems 2010, pp. 362-364.
12. D. Shastri, A. Merla, P. Tsiamyrtzis, and I. Pavlidis, "Imaging facial signs of neurophysiological responses," IEEE Transactions on Biomedical Engineering 2009, 56, vol. 477-484.
13. P. Leonard, T. F. Beattie, P. S. Addison, and J. N. Watson, "Standard pulse oximeters can be used to monitor respiratory rate," Emergency Medicine Journal 2003, 20, pp. 524-525.
14. P. S. Addison, and J. N. Watson, "A novel time-frequency-based 3D Lissajous figure method and its application to the determination of oxygen saturation from the photoplethysmogram," Measurement Science and Technology 2004, 15: pp. 15-18.
15. D. Shastri, A. Merla, P. Tsiamyrtzis, and I. Pavlidis, "Imaging facial signs of neurophysiological responses," IEEE Transactions on Biomedical Engineering 2009, 56: pp. 477-484.
16. F. Bousefsaf, C. Maaoui, and A. Pruski, "Continuous wavelet filtering on webcam photoplethysmographic signals to remotely assess the instantaneous heart rate," Biomedical Signal Processing and Control 2013, 8(Suppl 6), pp. 568-574.